THE JOURNAL OF BIOLOGICAL CHEMISTRY
Vol. 278, No. 12, Issue of March 21, pp. 10594–10601, 2003
Printed in U.S.A.

The GAFa Domains of Rod cGMP-phosphodiesterase 6 Determine the Selectivity of the Enzyme Dimerization*

Received for publication, August 19, 2002, and in revised form, January 9, 2003
Published, JBC Papers in Press, January 16, 2003, DOI 10.1074/jbc.M208456200

Khakim G. Muradov‡, Kimberly K. Boyd‡, Sergio E. Martinez§, Joseph A. Beavo§, and Nikolai O. Artemyev‡¶

From the ‡Department of Physiology and Biophysics, University of Iowa College of Medicine, Iowa City, Iowa 52242 and the §Department of Pharmacology, University of Washington, Seattle, Washington 98195

Retinal rod cGMP phosphodiesterase (PDE6 family) is the effector enzyme in the vertebrate visual transduction cascade. Unlike other known PDEs that form catalytic homodimers, the rod PDE6 catalytic core is a heterodimer composed of α and β subunits. A system for efficient expression of rod PDE6 is not available. Therefore, to elucidate the structural basis for specific dimerization of rod PDE6, we constructed a series of chimeric proteins between PDE6$\alpha\beta$ and PDE5, which contain the N-terminal GAFa/GAFb domains, or portions thereof, of the rod enzyme. These chimeras were co-expressed in Sf9 cells in various combinations as His-, myc-, or FLAG-tagged proteins. Dimerization of chimeric PDEs was assessed using gel filtration and sucrose gradient centrifugation. The composition of formed dimeric enzymes was analyzed with Western blotting and immunoprecipitation. Consistent with the selectivity of PDE6 dimerization *in vivo*, efficient heterodimerization was observed between the GAF regions of PDE6α and PDE6β with no significant homodimerization. In addition, PDE6α was able to form dimers with the cone PDE6α' subunit. Furthermore, our analysis indicated that the PDE6 GAFa domains contain major structural determinants for the affinity and selectivity of dimerization of PDE6 catalytic subunits. The key dimerization selectivity module of PDE6 has been localized to a small segment within the GAFa domains, PDE6α-59–74/PDE6β-57–72. This study provides tools for the generation of the homodimeric $\alpha\alpha$ and $\beta\beta$ enzymes that will allow us to address the question of functional significance of the unique heterodimerization of rod PDE6.

Photoreceptor rod and cone cGMP phosphodiesterases (PDE6 [1] family) are the effector enzymes in the vertebrate visual transduction cascade. The cascade is initiated by photoexcitation of the visual receptor rhodopsin and leads to hydrolysis of intracellular cGMP by transducin-activated PDE6 (1, 2). PDE6 enzymes belong to a large superfamily of phosphodiesterases of cyclic nucleotides that are critical modulators of cellular levels of cAMP and cGMP. Currently, eleven PDE families have been identified in mammalian tissues based on primary sequence, substrate selectivity, and regulation (3, 4). Rod PDE6 is composed of two homologous catalytic α- and β-subunits of similar size and two copies of an inhibitory γ-subunit (1, 5–8). Cone PDE6 catalytic dimer is made up of two identical PDEα' subunits (9). A cone-specific inhibitory Pγ-subunit is highly homologous to the rod Pγ (10). The δ-subunit associates with soluble rod and cone PDEs. It interacts with the methylated prenylated C termini of PDE6 catalytic subunits and regulates the enzyme attachment to the membrane (11). The role of the PDE δ-subunit in phototransduction is not well-defined, although it may modify the activity of the cascade by uncoupling transducin and PDE (12).

PDE6 enzymes have catalytic domains of about 280 aa residues in the C-terminal part of the molecule, which is highly conserved among all known cyclic nucleotide phosphodiesterases (3, 4). The catalytic region of photoreceptor PDEs closely resembles the catalytic site of cGMP binding, cGMP-specific PDE (PDE5) (45–48% sequence identity) (13). Furthermore, PDE6 and PDE5 share a strong substrate preference for cGMP and have similar patterns of inhibition by competitive inhibitors, including zaprinast, dipyridamole, and sildenafil (13–15). In addition to the C-terminal catalytic domain, PDE6 contains two N-terminal GAF domains (GAFa and GAFb). GAF domains have been recognized as a large family of domain homologues and named for their presence in cGMP-regulated PDEs, adenylyl cyclases, and the *E. coli* protein FhlA (16). Besides PDE6, several other PDE families possess GAF domains, including cGMP-stimulated PDE (PDE2), PDE5 (13, 17, 18), PDE10 (19), and PDE11 (20). At least one of the two GAF domains in the PDE2, PDE5, and PDE6 catalytic subunits serves as a site for noncatalytic binding of cGMP. Noncatalytic cGMP binding to GAF domains affects the catalytic properties of PDE2 and PDE5 (21–24). In PDE6, noncatalytically bound cGMP appears to enhance the affinity of the inhibitory interaction between Pγ and the catalytic core (25, 26). The second major function of the GAF domains is their role in dimerization of the PDE catalytic subunits. Earlier biochemical studies of PDE2 and PDE5 indicated that their dimerization occurs within the N-terminal parts of the molecules (18, 27). Ultimate evidence on the intersubunit interface of PDE2 has been recently provided by a solution of the crystal structure of PDE2A GAFa-GAFb domains (28). The crystal structure revealed that the PDE2A regulatory region forms a dimer with the interface formed by the two GAFa domains (28). The role of PDE6 GAF domains in dimerization is supported by recent electron microscopy imaging of rod PDE6$\alpha\beta$ (29). The imaging showed that the main intersubunit interaction occurs between the very N-terminal

* This work was supported in part by National Institutes of Health (NIH) Grant EY-10843. The services provided by the Diabetes and Endocrinology Research Center of the University of Iowa were supported by NIH Grant DK-25295. The costs of publication of this article were defrayed in part by the payment of page charges. This article must therefore be hereby marked "*advertisement*" in accordance with 18 U.S.C. Section 1734 solely to indicate this fact.

¶ Established Investigator of the American Heart Association. To whom correspondence should be addressed. Tel.: 319-335-7864; Fax: 319-335-7330; E-mail: nikolai-artemyev@uiowa.edu.

[1] The abbreviations used are: PDE, cGMP phosphodiesterase; Pγ, γ subunit of PDE6; PDE6α', α' subunit of cone PDE6; PDE5, cGMP-binding, cGMP-specific PDE (PDE5 family); aa, amino acid(s); IP, immunoprecipitation; FPLC, fast-protein liquid chromatography.

domains, presumably involving GAFa modules, and indicated that the GAFb domains may also contribute to the interface.

Almost all PDEs known to date are dimeric. However, the role of dimerization in enzyme function is not understood. Dimerization is not required for catalytic activity, because the isolated monomeric catalytic domain of PDE5 (30) and the monomeric short splice variant PDE4D2 (31) have been shown to be catalytically active. Furthermore, a majority of PDEs, with a notable exception of rod PDE6$\alpha\beta$, form catalytic homodimers (3, 4). Although the possibility of minor homodimeric species, $\alpha\alpha$ and $\beta\beta$, has not been ruled out, the dominant catalytic species of rod PDE6 is clearly a heterodimer $\alpha\beta$ (32, 33). The functional significance of heterodimerization of rod PDE remains unclear. It is as yet unknown if the catalytic characteristics of PDE6α and PDE6β in the dimer are equivalent. To circumvent the problem of a lack of efficient expression of PDE6 in various cell types (34, 35), we have previously developed a robust system for expression of PDE6α'/PDE5 chimeras in insect cells (36). In this study, we extended this approach to chimeras between PDE6$\alpha\beta$ and PDE5 to investigate the structural basis for specific dimerization of the rod PDE6 catalytic subunits. A series of chimeric proteins between PDE6 and PDE5 have been constructed that contain the GAFa and/or GAFb domains of PDE6 or PDE5. These chimeras were expressed in Sf9 cells in various combinations as His-, myc-, or FLAG-tagged proteins. The dimerization of chimeric PDE6 subunits was assessed using gel filtration, sucrose gradient centrifugation, Western blotting, and immunoprecipitation with anti-FLAG- and anti-myc-specific antibodies. The patterns of dimerization of chimeric PDE6/PDE5 subunits are consistent with the selectivity of PDE6 dimerization in rod photoreceptor cells. Our results indicate that the PDE6 GAFa domains contain major structural determinants for the affinity and selectivity of dimerization of PDE6 catalytic subunits.

EXPERIMENTAL PROCEDURES

Materials—cGMP was obtained from Roche Molecular Biochemicals. [^{3}H]cGMP was a product of Amersham Biosciences. All restriction enzymes were purchased from New England BioLabs. AmpliTaq® DNA polymerase was a product of PerkinElmer Life Sciences, and *Pfu* DNA polymerase was a product of Stratagene. All other reagents were purchased from Sigma. Bovine holo-PDE6 was extracted from bleached rod outer segment membranes and purified as described previously (33).

Cloning, Expression, and Purification of PDE6/PDE5 Chimeras—To construct PDE6α/PDE5 chimera FLAG-α-α-5 (see Fig. 1), the FLAG tag DNA sequence was first inserted into the pFastBacHTb vector (Invitrogen) replacing the His6 sequence. A DNA fragment was PCR-amplified using pFastBacHTb as a template, a 5′-primer containing an *Rsr*II site and the FLAG tag sequence, and a 3′-primer containing a *Bam*HI site. This fragment was then ligated with the large *Rsr*II/*Bam*HI fragment of pFastBacHTb to produce pFastBacFLAG. A bovine retinal cDNA library kindly provided by Dr. W. Baehr (University of Utah) was used as a template for PCR amplifications of PDE6$\alpha\beta$ sequences. DNA coding for PDE6α-1–443 was PCR-amplified using primers carrying *Bam*HI and *Hin*dIII sites. DNA coding for PDE5–506-865 amino acids was PCR-amplified using the pFastBacHTb-PDE5 template (36) and primers with the *Hin*dIII and *Xho*I sites. The two PCR products were ligated into the pFastBacFLAG vector using the *Bam*HI and *Xho*I sites. The myc tag DNA sequence was inserted into the pFastBacHTb vector using a PCR-directed cloning procedure similar to the insertion of the FLAG tag sequence. The construct for chimera myc-β-β-5 (see Fig. 1) was generated by ligation of the PCR-amplified PDE6β-1–441 and PDE5–506-865 DNAs into the *Bam*HI and *Xho*I sites of pFastBacmyc.

The His-tagged PDE6$\alpha\beta$/PDE5 chimeras were constructed by amplifying appropriate regions of the PDE6$\alpha\beta$ subunits with primers containing unique restriction sites. When unique restriction sites were not available at the desired location, first-round PCR products coding chimeric junctions were extended to the nearest unique sites in a second-round PCR amplification. To improve the recognition of the His_6 tag by commercial antibodies, the His_6 flanking sequence in the original pFastBacHTb vector was replaced by the His_6 flanking sequence from pET-15b (Novagen). The DNA sequences of all constructs were confirmed by automated DNA sequencing at the University of Iowa DNA core facility.

Generation of the recombinant bacmids, transfection of Sf9 cells, and viral amplifications were carried out according to the manufacturer's recommendations (Invitrogen). For protein expression, Sf9 cell cultures (10 ml, 2×10^6 cells/ml) were infected with one or two different viruses at a multiplicity of infection of 3–10. Sf9 cells were harvested at 48 h after infection by centrifugation and stored at −80 °C until use. Sf9 cells were resuspended in 3 ml of 20 mM Tris-HCl buffer (pH 8.0) containing 2 mM $MgSO_4$ and Complete™ Mini protease inhibitor mixture (one-third tablet) (Roche Molecular Biochemicals) and sonicated with two 10-s pulses using a microtip attached to a 550 Sonic Dismembrator (Fisher Scientific). Sf9 cell lysates were cleared by centrifugation (100,000 × *g*, 90 min, 2 °C), dialyzed against 30 mM Tris-HCl buffer (pH 8.0) containing 130 mM NaCl, 2 mM $MgSO_4$, and 50% glycerin, and then centrifuged again at 100,000 × *g* for 1 h at 2 °C. Dialysis against 50% glycerin allowed a concentration of PDE samples by ~4-fold and subsequent storage at −20 °C without freezing. The presence of glycerin did not affect the behavior of PDEs in gel filtration.

Gel Filtration and Fraction Analysis—Aliquots of dialyzed PDE samples (50–200 μl) were injected into a Superose® 12 10/30 column (Amersham Biosciences) equilibrated at 25 °C with 30 mM Tris-HCl buffer (pH 8.0) containing 100 mM NaCl and 2 mM $MgSO_4$. Proteins were eluted at 0.4 ml/min, and 0.4-ml fractions were collected starting at 17 min post-injection. Each fraction was assayed for PDE activity, protein concentration, and the presence of chimeric PDEs by Western blotting. PDE activity was measured using 10- to 20-μl aliquots from fractions and 5 μM [^{3}H]cGMP as described previously (37, 38). Protein concentrations were determined by the method of Bradford using IgG as a standard (39). The column was calibrated with the following protein standards: bovine thyroglobulin (670 kDa, 85 Å), horse ferritin (440 kDa, 61 Å), sweet potato β-amylase (200 kDa), rabbit aldolase (158 kDa, 48.1 Å), bovine serum albumin (67 kDa, 35.5 Å), and chicken ovalbumin (45 kDa, 30.5 Å). The Stokes radii for PDEs were estimated using the correlation of elution volume with the Stokes radius proposed by Porath (40). Gel filtration analyses were performed two or more times with similar results for each PDE chimera combination from at least two different preparations of Sf9 cell extracts. Results of a typical analysis are shown.

Western blot analysis of the gel filtration fractions (20-μl aliquots) was performed following SDS-PAGE in 10% gels (41). Monoclonal anti-polyhistidine, M2 monoclonal anti-FLAG, and monoclonal anti-c-myc (clone 9E10) antibodies (Sigma) with the respective dilutions of 1:1500, 1:5000, and 1:5000 were utilized. The antibody·antigen complexes were detected using anti-mouse antibodies conjugated to horseradish peroxidase (Sigma) and ECL reagent (Amersham Biosciences). The compositions of PDE complexes in fractions corresponding to dimeric enzymes were examined by immunoprecipitation (IP). Aliquots of the gel filtration fractions (80 μl) were incubated with or without anti-FLAG or myc-antibodies (1 μl) for 30 min at 25 °C followed by the addition of 5 μl of protein G-Agarose (Sigma) and incubation for 40 min at 25 °C. The agarose beads were washed four times with 300 μl of phosphate-buffered saline (pH 7.1), and the bound proteins were eluted with an SDS-PAGE sample buffer. PDE complexes were separated on 10% gels and analyzed by Western blotting using appropriate antibodies.

Sucrose Gradient Centrifugation—Sucrose density gradients (5–35%) were prepared in 30 mM Tris-HCl (pH 8.0) buffer containing 100 mM NaCl, 2 mM $MgSO_4$, and 4 mM 2-mercaptoethanol using a Gradi-Frac gradient former (Amersham Biosciences). Protein standards or aliquots of 200 μl from peak PDE gel filtration fractions were loaded onto the gradients in 14- × 89-mm centrifugation tubes and centrifuged for 24 h at 40,000 rpm in a Beckman SW41 rotor at 4 °C. Fractions of 300 μl were collected starting from the bottom of the tubes. Fractions from the tubes with protein standards were analyzed for protein concentration, whereas fractions from the tubes containing PDE samples were analyzed for PDE activity. Sucrose density centrifugations were performed two times with similar results for each PDE preparation. Results of a typical analysis are shown. The protein standards were: bovine liver catalase (250 kDa, 11.3 S), rabbit aldolase (158 kDa, 7.3 S), bovine serum albumin (67 kDa, 4.6 S), and chicken ovalbumin (45 kDa, 3.5 S). Sedimentation coefficients ($s_{20,w}$) for chimeric PDEs were estimated using a linear plot of distances traveled by standards from meniscus *versus* the $s_{20,w}$ values of standards (42). The molecular weights of PDEs were calculated using the estimated sedimentation coefficients, the Stokes radii obtained from the gel filtration data, and the following equation (43),

$$M = (s \cdot N_A \cdot 6 \cdot \pi \cdot \eta \cdot r)/(1 - v \cdot \rho) \quad \text{(Eq. 1)}$$

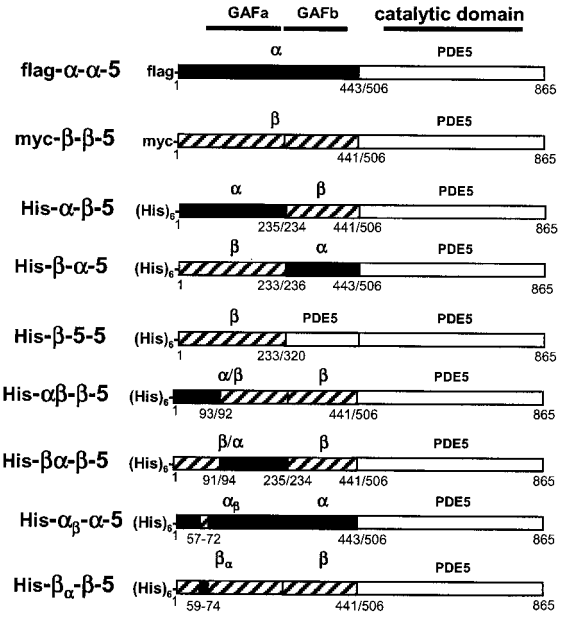

FIG. 1. **Schematic representation of PDE6/PDE5 chimeras.** Constructs are designated as follows: name of tag, composition of GAFa domain, composition of GAFb domain, catalytic domain. Subscripts α and β indicate replacements PDE6α-59–74 and PDE6β-57–72 within the PDE6β and PDE6α GAF regions, respectively.

where s is the sedimentation coefficient; N_A is Avogardo's number; η is the viscosity of the medium (0.01 g·cm^{-1}·s^{-1}), r is the Stokes radius; v is the partial specific volume of a protein (0.73 cm^3·g^{-1}), and ρ is the density of the medium (1 g·cm^{-3}).

RESULTS

Selectivity of Dimerization of the GAFa-GAFb Domains of Rod PDE6—Dimerization of PDE6 catalytic subunits is very tight, and, apparently, there is no exchange of subunits between dimers once they are formed following the synthesis and folding of the polypeptide chains. The dimer formation between chimeric PDE6/PDE5 subunits was therefore assessed following co-expression of these chimeras in Sf9 cells. Chimeric PDEs (Fig. 1) from soluble fractions of Sf9 cells as well as native PDE6 and recombinant wild-type PDE5 were examined by FPLC gel filtration on a calibrated Superose 12 HR 10/30 column and by sucrose gradient centrifugation. The elution profiles of native PDE6 and recombinant wild-type PDE5 on the gel filtration column were very similar and corresponded to an apparent molecular mass of ~210 kDa (Fig. 2*A*), which is consistent with dimerization of the catalytic subunits. Molecular masses of rod holoPDE6 (PDE$\alpha\beta\gamma_2$) and the PDE5 dimer calculated from the sequences were ~217 and 197 kDa, respectively. Only relatively small fractions of the enzymes (~15% PDE5 and ~10% PDE6) migrated as aggregates with high molecular mass. The previously developed chimeric PDE, Chi4 (termed hereafter His-α'-α'-5), containing the cone PDE6α' GAFa-GAFb region and the catalytic domain of PDE5 (36), is predicted to form homodimers. The chromatographic behavior of His-α'-α'-5 on a Superose 12 HR 10/30 column indicated an apparent molecular mass of ~200 kDa (Fig. 2*A*), which is in good agreement with the theoretical molecular mass of 183 kDa for the α'-α'-5 homodimer. The fraction of aggregates in the chimeric PDE (~10%) was similar to those in PDE5 and PDE6 preparations.

We first constructed PDE6/PDE5 chimeras containing both the GAFa and GAFb domains from either rod PDE6α (α-α-5) or PDE6β (β-β-5) and the catalytic domain from PDE5 (Fig. 1). As generally defined by the PDE sequence alignment and the crystal structure (17, 28), the boundaries of the GAFa domains

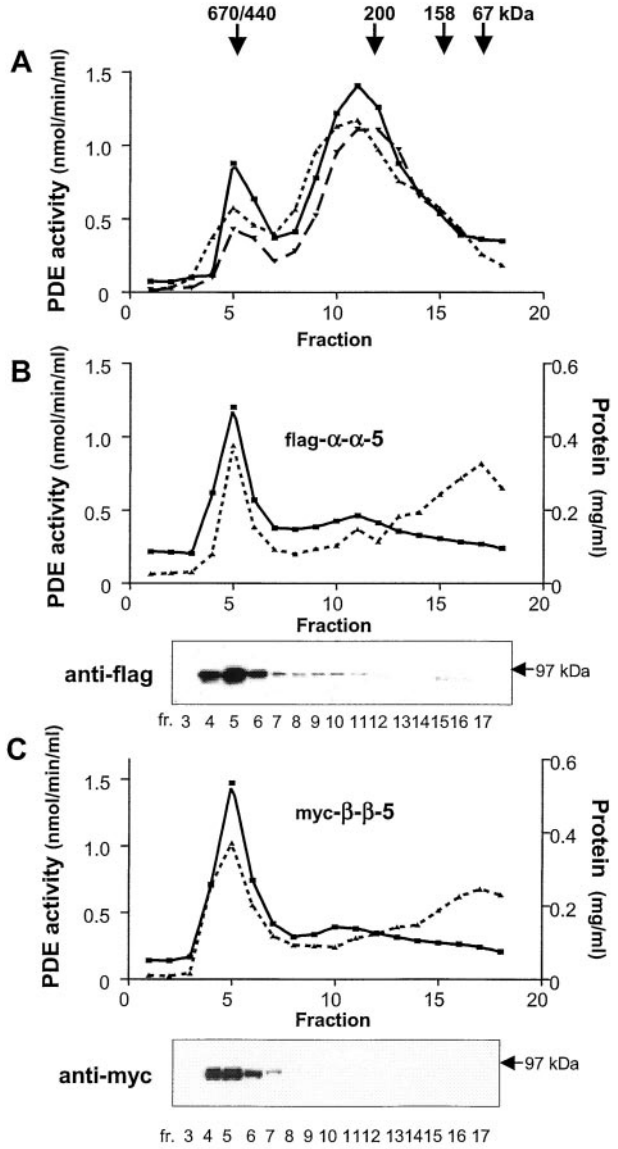

FIG. 2. **Gel filtration profiles of PDE5, PDE6, and chimeric PDEs α'-α'-5, α-α-5, and β-β-5.** *A*, rod holoPDE6 (50 μg) (*smaller dashed line*) mixed with the dialyzed cell extract of noninfected Sf9 cells (100 μl) or dialyzed cell extracts of Sf9 cells (100,000 × *g*, 90 min) infected with viruses for expression of PDE5 (50 μl) (*solid line*) and α'-α'-5 (100 μl) (*larger dashed line*) were subjected to FPLC gel filtration on a Superose® 12 10/30 column (Amersham Biosciences). Fractions of 0.4 ml were collected and analyzed for PDE activity. *B* and *C*, chimeras FLAG-α-α-5 (*B*) and myc-β-β-5 (*C*) were expressed individually in Sf9 cells and the dialyzed soluble cell extracts (100,000 × *g*, 90 min) were subjected to FPLC gel filtration. Fractions of 0.4 ml were collected and analyzed for protein concentration (*dashed line*), PDE activity (*solid line*), and by Western blotting with anti-FLAG or anti-myc antibodies.

are PDE6α-54–220 and PDE6β-52–218, and the boundaries of the GAFb domains are PDE6α-255–443 and PDE6β-253–441. The nonconserved N termini, PDE6α-1–53 in α-α-5 and PDE6β-1–51 in β-β-5, were from the respective catalytic subunits. Chimera α-α-5 was constructed for expression as a FLAG-tagged protein, whereas β-β-5 was generated as a myc-tagged polypeptide. Gel filtration fractions were analyzed by Western blotting for the presence of chimeric PDE proteins and for PDE activity with cGMP as the substrate. Individual expression of FLAG-α-α-5 or myc-β-β-5 resulted in the formation of only high molecular weight aggregates that migrated with the exclusion volume of the Superose 12 column (Fig. 2, *B* and

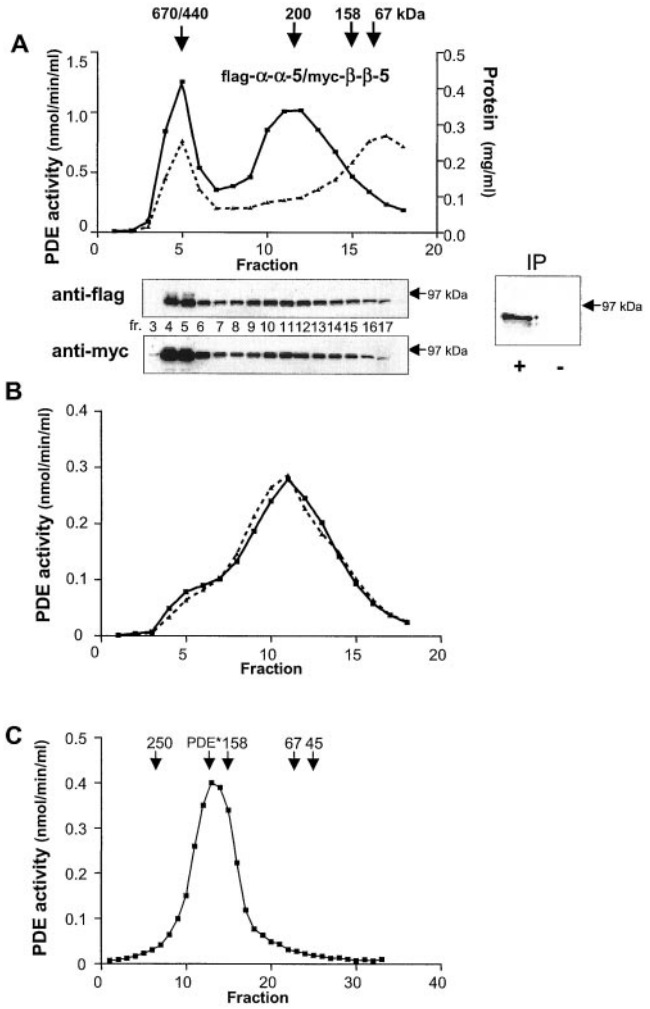

FIG. 3. **Analysis of dimerization of PDE chimeras α-α-5 and β-β-5.** *A*, chimeras FLAG-α-α-5 and myc-β-β-5 were co-expressed in Sf9 cells and examined by gel filtration on the Superose® 12 column. Fractions of 0.4 ml were collected and analyzed for protein concentration (*dashed line*), PDE activity (*solid line*), and by Western blotting with anti-FLAG or anti-myc antibodies. *IP*, an aliquot (80 μl) of the dimeric PDE peak fraction 12 was incubated with (+) or without (−) anti-FLAG antibodies. Protein·antibody complexes were isolated using protein G-agarose and analyzed by Western blotting with anti-myc as described under "Experimental Procedures." *B*, combined PDE peak front fractions 9–11 (*solid line*) and tail fractions 13–16 (*dashed line*) were concentrated by dialysis against 30 mM Tris-HCl buffer (pH 8.0) containing 130 mM NaCl, 2 mM $MgSO_4$, and 50% glycerin and then reapplied onto the column. *C*, combined peak PDE gel filtration fractions 10–13 were concentrated to a volume of 200 μl using the YM-10 Microcon® devices (Millipore Corp., Bedford, MA) and loaded onto the 5–35% sucrose density gradients. Following centrifugation for 24 h at 40,000 rpm in a Beckman SW41 rotor, fractions of 300 μl were collected starting from the bottom of the tubes and analyzed for PDE activity. *Arrows* indicate sedimentation of protein standards. PDE5, holoPDE6, and α′-α′-5 migrated at the same position of the gradient indicated as *PDE**.

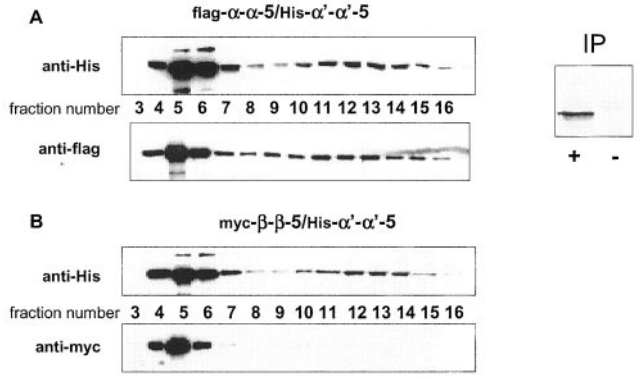

FIG. 4. **Analysis of dimerization of PDE chimeras α-α-5 and β-β-5 with α′-α′-5.** His-α′-α′-5 was co-expressed with FLAG-α-α-5 (*A*) or myc-β-β-5 (*B*) in Sf9 cells. Soluble Sf9 cell extracts (100,000 × *g*, 90 min) were applied onto a FPLC Superose® 12 10/30 gel filtration column. Aliquots (20 μl) from 0.4-ml gel filtration fractions were analyzed by Western blotting with anti-His, anti-FLAG, or anti-myc antibodies. *IP*, an aliquot (80 μl) of the dimeric FLAG-α-α-5·His-α′-α′-5 peak fraction 12 was incubated with (+) or without (−) anti-FLAG antibodies. Protein·antibody complexes were isolated using protein G-agarose and analyzed by Western blotting with anti-His as described under "Experimental Procedures."

C). Furthermore, the aggregates also migrated with the exclusion volume on a Superose 6 HR 10/30 column (not shown), which is capable of separating proteins weighing up to 1×10^6 kDa. Notably, these aggregates were capable of hydrolyzing cGMP. When FLAG-α-α-5 and myc-β-β-5 were co-expressed in Sf9 cells, a peak of PDE activity appeared in the fractions corresponding to dimeric PDE species with an apparent molecular mass of ~200 kDa (Fig. 3*A*). Approximately 50% of the total soluble FLAG/myc-tagged protein formed the dimeric enzyme. In the peak activity fractions 11 and 12, the enzyme hydrolyzed cGMP with a K_m value of 3.8 μM and a V_{max} of 21 nmol/min/mg of protein. The Western blot analysis of these fractions using anti-FLAG and anti-myc antibodies confirmed the presence of both FLAG-α-α-5 and myc-β-β-5 (Fig. 3*A*). A sizable peak of PDE activity was also present in fractions corresponding to aggregates of FLAG-α-α-5 and myc-β-β-5 (Fig. 3*A*). The aggregation appears to be irreversible, because rechromatography of the fractions with aggregates did not generate dimeric enzymes (not shown). Considering the intensity of immunostaining, the catalytic activity of these aggregated PDE species is 1.5- to 2-fold lower than that of the dimeric PDE species.

To verify the nature of the dimeric species, chimeric PDE was immunoprecipitated with anti-FLAG antibodies and then probed with anti-myc antibodies using Western blotting. The results of the IP experiments proved the formation of a heterodimer between FLAG-α-α-5 or myc-β-β-5 (Fig. 3*A*). The peak of dimeric PDE activity on the gel filtration column was relatively broad. To determine if this PDE might be heterogeneous, the combined concentrated front fractions 9–11 and tail fractions 13–16 were reapplied onto the column. The resulting PDE activity profiles were nearly identical, suggesting the presence of a single dimeric form of PDE and trace amounts of aggregates (Fig. 3*B*).

The molecular shape of a protein significantly influences its migration on a gel filtration column. Sucrose density centrifugation was utilized as an additional independent approach to estimate the molecular weight of chimeric PDEs (42). The sedimentation rates of native rod holoPDE6, recombinant PDE5, His-α′-α′-5, and the FLAG-α-α-5·myc-β-β-5 complex were similar (Fig. 3*C*). An estimated $s_{20,w}$ value of 8.1 for the FLAG-α-α-5·myc-β-β-5 complex corresponds well to the dimeric structure. Using this sedimentation coefficient and the Stokes radius of 52 Å derived from the gel filtration data (Fig. 3*A*) (40), Equation 1 (43) yields a molecular mass of 176 kDa, which is comparable to the theoretical molecular mass (184 kDa) for the FLAG-α-α-5·myc-β-β-5 dimer.

Next, we examined the possibility of dimerization of PDE6α and PDE6β with cone PDE6α′ and PDE5. FLAG-α-α-5 and myc-β-β-5 each were co-expressed with His-α′-α′-5 or His-PDE5. Because PDE6α′ and PDE5 form catalytic homodimers, a peak of PDE activity in gel filtration fractions corresponding to dimeric PDE species cannot be used as evidence for heterodimerization. Instead, we relied on Western blot analysis of

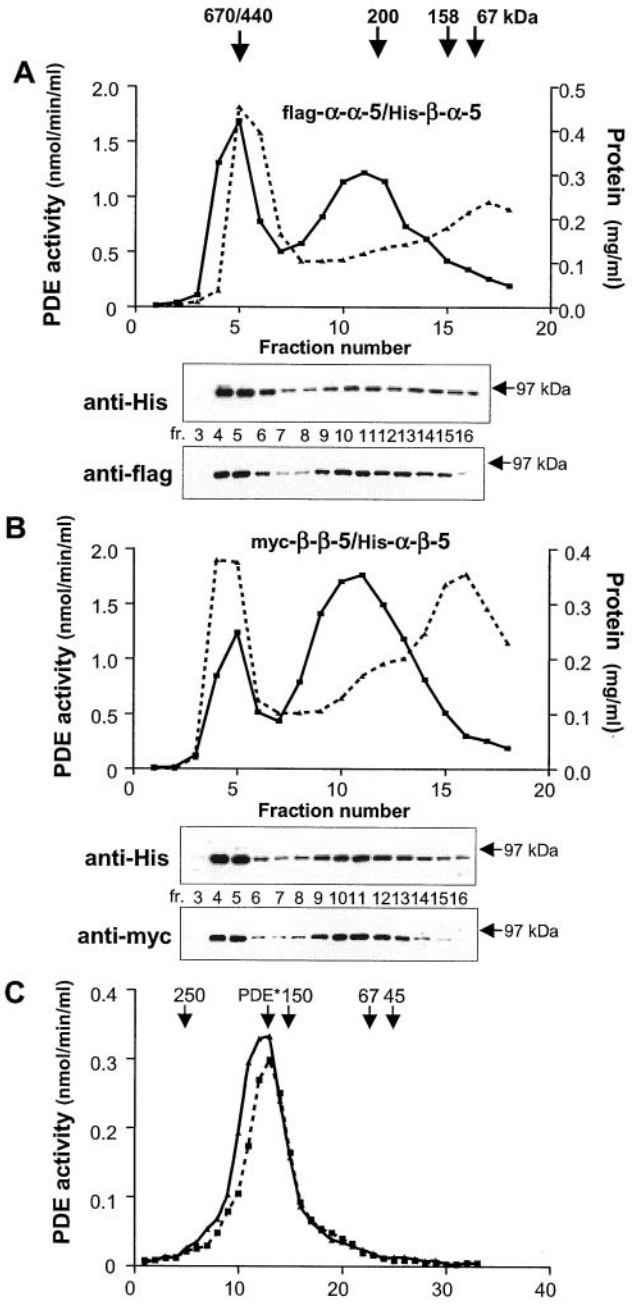

FIG. 5. **Dimerization of β-α-5 with α-α-5 and α-β-5 with β-β-5.** *A* and *B*, combinations of chimeras, FLAG-α-α-5·His-β-α-5 (*A*) and myc-β-β-5·His-α-β-5 (*B*), were co-expressed in Sf9 cells and analyzed by FPLC gel filtration on a Superose® 12 10/30 column (*dashed line*, protein concentration; *solid line*, PDE activity) and Western blotting using anti-His, anti-FLAG, or anti-myc antibodies as described under "Experimental Procedures." *C*, combined peak FLAG-α-α-5·His-β-α-5 (*dashed line*) and myc-β-β-5·His-α-β-5 (*solid line*) gel filtration fractions 10–13 were concentrated to a volume of 200 μl using the YM-10 Microcon® devices (Millipore Corp., Bedford, MA) and loaded onto the 5–35% sucrose density gradients. Following centrifugation for 24 h at 40,000 rpm in a Beckman SW41 rotor, fractions of 300 μl were collected starting from the bottom of the tubes and analyzed for PDE activity.

the fractions for the presence of FLAG-α-α-5 and myc-β-β-5. The Western blot analysis of the gel filtration fractions of PDE species formed upon co-expression of FLAG-α-α-5 and His-α′-α′-5 indicated heterodimerization between the two subunits (Fig. 4*A*). The FLAG-α-α-5 signal appeared in fractions 10–14 corresponding to dimeric PDE. The immunoprecipitates of these fractions with anti-FLAG antibodies contained His-α′-α′-5, demonstrating the heterodimeric composition of the

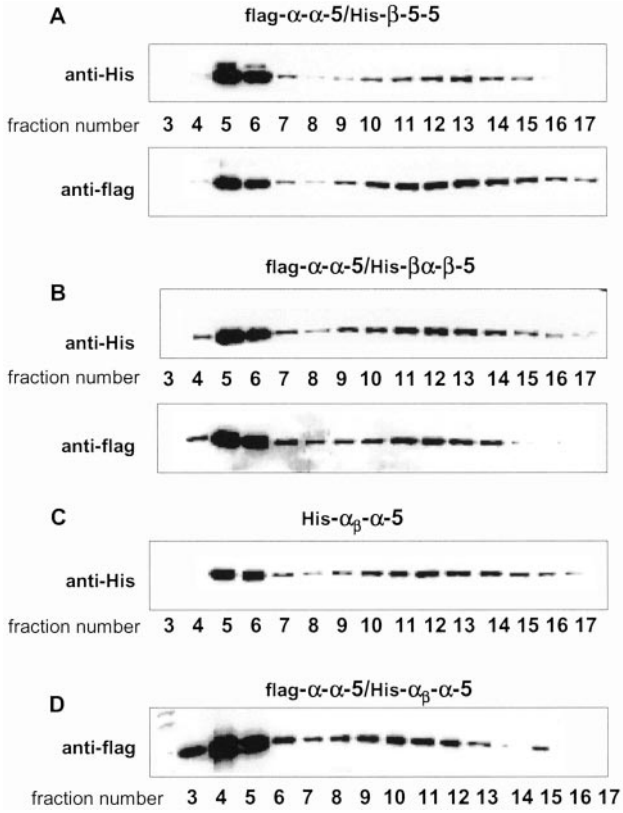

FIG. 6. **Dimerization of α-α-5 with β-5–5, βα-β-5, or α$_β$-α-5.** Chimera FLAG-α-α-5 was co-expressed with His-β-5–5 (*A*), His-βα-β-5 (*B*), or His-α$_β$-α-5 (*D*) in Sf9 cells. Chimera His-α$_β$-α-5 alone was expressed in Sf9 cells to test its capacity for homodimerization (*C*). Dimer formation was examined by the Western blot analysis of the fractions following separation of the chimeric PDEs on a Superose® 12 10/30 column.

dimers (Fig. 4*A*). Co-expression of myc-β-β-5 and His-α′-α′-5 has not led to any significant dimer formation between the two chimeric PDEs (Fig. 4*B*). Similarly, co-expression of FLAG-α-α-5 or myc-β-β-5 with PDE5 and examination of formed PDE species revealed no detectable dimerization between the GAF regions of rod PDE6 and PDE5 (not shown). The patterns of dimerization α-α-5 or β-β-5 were consistent with the selectivity of PDE6 dimerization in rod photoreceptor cells, allowing us to use them as templates to further probe the role of the PDE6 GAFa and GAFb domains.

Roles of the GAFa and GAFb Domains in Rod PDE6 Dimerization—To determine the contributions of the rod PDE6 GAFa and GAFb domains to the enzyme dimerization, two new PDE6/PDE5 chimeras have been constructed. Chimera His-α-β-5 contained the GAFa and GAFb domains from PDE6α and PDE6β, respectively (Fig. 1). The GAF domains were swapped in the second chimera, His-β-α-5. If the rod PDE6 catalytic subunits associate in a symmetrical "head-to-tail" fashion, His-α-β-5 and His-β-α-5 might have been capable of self-dimerization. However, the gel filtration and Western blot analyses of His-α-β-5 and His-β-α-5 expressed individually in Sf9 cells revealed no formation of dimeric PDEs (not shown). In contrast, catalytically active dimeric PDE species were observed following co-expression of His-α-β-5 and His-β-α-5 (not shown), suggesting a "head-to-head" dimerization of the PDE6α and PDE6β subunits. The lack of self-dimerization of FLAG-α-α-5, myc-β-β-5, His-α-β-5, and His-β-α-5 allowed us to probe the role of the GAFa and GAFb domains by co-expressing His-α-β-5 and His-β-α-5 with either FLAG-α-α-5 or myc-β-β-5. Two of the four combinations, FLAG-α-α-5·His-α-β-5 and myc-β-β-5·His-β-α-5, yielded no dimeric PDE species (not shown). The other two

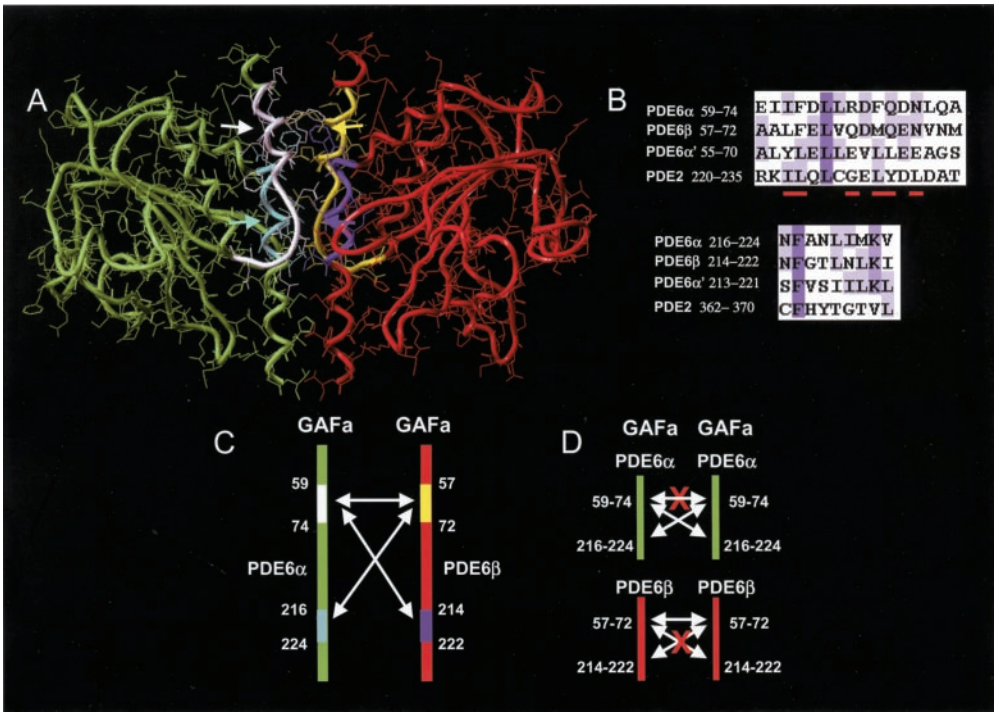

FIG. 7. **A model of the PDE6αGAFa-PDE6βGAFa dimer.** *A*, a homology model of the PDE6αGAFa-PDE6βGAFa dimer was generated with Swiss-PdbViewer (version 3.7b2) and SWISS-MODEL (44) using the coordinates of the PDE2A GAFa-GAFb dimer as a template (28). The image was produced using Sybyl (version 6.6, Tripos). The PDE6αGAFa and PDE6βGAFa domains are shown in *green* and *red*, respectively. Putative intersubunit contact regions PDE6α-59–74 (*white*), PDE6α-216–224 (*cyan*), PDE6β-57–72 (*yellow*), and PDE6β-214–222 (*blue*) are indicated by *arrows*. *B*, sequence alignments (45) of the PDE6 α, β, α′ and PDE2 segments corresponding to PDE6α-59–74 and PDE6α-216–224. PDE2 intersubunit contact residues within PDE2–220-235 are *underlined*. *C*, from the model, PDE6α-59–74 (*white*) interacts with PDE6β-57–72 (*yellow*) and PDE6β-214–222 (*blue*), and PDE6β-57–72 interacts with PDE6α-59–74 and PDE6α-216–224 (*cyan*). *D*, schematic depiction of probable interaction defects excluding homodimerization of PDE6α and PDE6β.

TABLE I
Summary of dimerization properties of PDE6/PDE5 chimeras
See Fig. 1 for composition of the PDE chimeras.

Combinations of chimeras forming dimeric PDEs[a]	Combinations of chimeras unable to form dimeric PDEs
α-α-5/β-β-5 (3.8)[b]	α-α-5/PDE5; β-β-5/PDE5; β-β-5/α′-α′-5
α-α-5/α′-α′-5 (ND) α-β-5/β-α-5 (5.2)	α-α-5/α-β-5; β-β-5/β-α-5
α-α-5/β-α-5 (2.7)	β-β-5/β-5-5; α-α-5/5-β-5; β-β-5/5-β-5
β-β-5/α-β-5 (4.9)	α-α-5/αβ-β-5; β-β-5/αβ-β-5
α-α-5/β-5-5 (2.3)	β-β-5/βα-β-5; αβ-β-5/βα-β-5
α-α-5/βα-β-5 (4.5) βα-β-5/α-β-5 (4.2)	β-β-5/α_{β}-α-5
α-α-5/α_{β}-α-5 (ND) α_{β}-α-5/α_{β}-α-5 (3.4)	α-α-5/β_{α}-β-5; β-β-5/β_{α}-β-5

[a] Except for α_{β}-α-5 and α′-α′-5, all constructed PDE chimeras did not form homodimeric species.
[b] K_m values (μM); *ND*, K_m values are not determined due to homodimerization of α′-α′-5 or α_{β}-α-5.

combinations, FLAG-α-α-5·His-β-α-5 and myc-β-β-5·His-α-β-5, produced functional dimeric enzymes as evidenced from the gel filtration and sucrose density centrifugation data (Fig. 5). The migrations of FLAG-α-α-5·His-β-α-5 and myc-β-β-5·His-α-β-5 in gel filtration and in the sucrose density gradient were similar to those of the FLAG-α-α-5·myc-β-β-5 complex. The catalytic characteristics of FLAG-α-α-5·His-β-α-5 (K_m = 2.7 μM, V_{max} = 20 nmol/min/mg) and myc-β-β-5·His-α-β-5 (K_m = 4.9 μM, V_{max} = 17 nmol/min/mg) assayed in the peak fractions #11 (Fig. 5, *A* and *B*) were comparable to those of FLAG-α-α-5·myc-β-β-5. The results of these experiments suggest that the main selectivity determinants of dimerization of PDE6α and PDE6β reside within the GAFa domains.

The GAFb domains of PDE6α and PDE6β are more homologous than the GAFa domains and may contribute to the affinity of dimerization without influencing its selectivity. Chimera His-β-5–5 containing the GAFa domain of PDE6β and the GAFb domain of PDE5 was generated to test this possibility. His-β-5–5 did not exhibit any propensity for self-dimerization (not shown) but was able to efficiently form heterodimers with FLAG-α-α-5 when the two proteins were co-expressed in Sf9 cells (Fig. 6*A*). Sucrose density centrifugation of FLAG-α-α-5·His-β-5–5 produced a $s_{20,w}$ value of 8.1 confirming the dimeric nature of the complex (not shown). Therefore, the GAFb domains of PDE6 do not significantly contribute to the dimeric interface.

Mapping Dimerization Selectivity Determinants within the GAFa Domains of PDE6—The dimerization properties of His-α-β-5 and His-β-α-5 indicated that the major selectivity determinants are localized within PDE6α-1–235 (PDE6β-1–233). Approximately 45-residue-long N-terminal sequences of the PDE6 α, β, and α′ subunits are very dissimilar and are followed by modestly conserved N-terminal portions of the GAFa domains (~aa 45–90). The degree of conservation between the GAFa domains is higher in the remaining GAFa segments (~aa 90–230). This was taken into consideration in designing chimeras His-αβ-β-5 and His-βα-β-5 (Fig. 1). His-αβ-β-5 and His-βα-β-5 included the PDE6α sequences 1–93 and 94–235, respectively, substituting corresponding sequences of PDE6β. After His-αβ-β-5 and His-βα-β-5 showed no capacity for self-dimerization, these chimeras were co-expressed with FLAG-α-α-5 or myc-β-β-5. The combinations FLAG-α-α-5·His-αβ-β-5, myc-β-β-5·His-αβ-β-5, or myc-β-β-5·His-βα-β-5 produced no dimeric PDE species as judged by the gel filtration and Western blot analysis (not shown). On the contrary, His-βα-β-5 and FLAG-α-α-5 were capable of assembly of catalytically active dimeric PDE (Fig. 6*B*). Sedimentation of FLAG-α-α-5·His-βα-β-5 in the sucrose gradient ($s_{20,w}$ 8.1) and the K_m value for

cGMP hydrolysis (4.5 μM) were equivalent to the properties of other chimeric PDEs. In addition, His-$\beta\alpha$-β-5 formed dimers with His-α-β-5 (not shown). These data indicate that at least some PDE6$\alpha\beta$ dimerization selectivity determinants are localized to within ~90 N-terminal residues of the PDE6 α and β subunits.

The major role of the GAFa domains in the dimerization of both PDE2 (28) and PDE6 suggests similar topographies of the intersubunit interfaces. The structure of the PDE2 (GAFa-GAFb)$_2$ dimer shows two main sites in each monomer that participate in the intersubunit interface, one comprising a portion of the α-helix 1 and the α1/α2 loop, and the second including the helix connecting GAFa and GAFb (28). On the basis of a homology model of the PDE6αGAFa-PDE6βGAFa dimer (Fig. 7, *A* and *B*), the former site corresponds to ~16 residue segments in PDE6α (aa 59–74) and PDE6β (aa 57–72), which are situated within the N-terminal 90-residue dimerization selectivity regions. Chimeras His-α_β-α-5 and His-β_α-β-5 (Fig. 1) have been constructed to test the possibility that these PDE6 α and β segments are responsible for the selectivity of PDE6 dimerization. Gel filtration tests (Fig. 6*C*) and sucrose density centrifugation (not shown) revealed that, unlike other constructed rod PDE6 chimeras (Table I), His-α_β-α-5 was able to form homodimers. His-α_β-α-5 and His-β_α-β-5 were then tested for the ability to form heterodimers with FLAG-α-α-5 or myc-β-β-5. Consistent with the role of PDE6α-59–74/PDE6β-57–72 as determinants for PDE6$\alpha\beta$ dimerization, His-α_β-α-5 failed to dimerize with myc-β-β-5, whereas His-β_α-β-5 did not produce dimers with FLAG-α-α-5 (not shown). Furthermore, although His-β_α-β-5 was unable to dimerize with myc-β-β-5 (not shown), His-α_β-α-5 displayed a gain of dimerization with FLAG-α-α-5 (Fig. 6*D*). The formation of FLAG-α-α-5·His-α_β-α-5 dimers was also confirmed using immunoprecipitation with anti-FLAG antibodies followed by Western blotting with anti-His antibodies (not shown).

DISCUSSION

The structural basis and functional role of PDE dimerization are poorly understood because dimerization is not required for catalytic function. The first molecular insights into PDE dimerization have been revealed by the structure of the regulatory domains of PDE2A (28). This crystal structure demonstrates that the GAFa domain is responsible for the dimerization of PDE2A. One apparent implication from the PDE2A structure is that other GAF domain-containing PDEs, such as PDE5, PDE6, PDE10, and PDE11 utilize GAF modules for dimerization. Yet, it remains unclear how well the dimerization interfaces of PDE5 and PDE6 parallel that of PDE2. Although at a relatively low resolution, electron microscopy imaging of PDE5 and PDE6 showed molecular shapes that are somewhat different from the PDE2 structure (29). Furthermore, the electron microscopy study indicates that, in addition to GAFa, GAFb domains may contribute to the intersubunit interaction in PDE5 and PDE6. Analysis of the dimerization interface of rod PDE6 catalytic subunits permitted us to address two unresolved questions. What are the key structural determinants for dimerization of PDE6, and are they similar to those identified in the PDE2A structure? What are the selectivity determinants of rod PDE6 heterodimerization? The heterodimerization of rod PDE6 α and β subunits is unique among known PDEs. It may be critical in the forming of rod-specific photoresponses. However, a potential significance of PDE6$\alpha\beta$ heterodimers and the properties of individual subunits cannot be assessed in the absence of $\alpha\alpha$ and $\beta\beta$ homodimers. Identification of the selectivity determinants would be a first major step toward generation of the homodimeric species.

Our analysis of dimerization of chimeric PDE6$\alpha\beta$/PDE5 proteins using gel filtration, immunoprecipitation, and sucrose gradient centrifugation demonstrated selective heterodimerization between the GAF regions of PDE6 α- and β-subunits with no significant homodimerization. This observation is in accordance with the established heterodimeric nature of the rod enzyme. Interestingly, the GAFa-GAFb region of PDE6α, but not PDE6β, was capable of forming a dimer with the GAFa-GAFb region of PDE6α'. Although dimerization of PDE6α and PDE6α' does not have physiological implications, as the subunits are expressed in different types of photoreceptor cells, it may provide additional clues to understanding PDE6 intersubunit interfaces. The patterns of dimerization (or lack thereof) (Table I) show that the GAFa domains are the major contributors to the dimer assembly of PDE. The finding that the PDE6 GAFa domains, similar to the PDE2 GAFa domains, are responsible for its dimerization suggests a common structural organization of the intersubunit interfaces of the GAF domain-containing PDEs.

The subsequent identification of the PDE6$\alpha\beta$ dimerization selectivity determinants was carried out using chimeras carrying complementing portions of the PDE6 α and β GAFa domains. The ability of His-$\beta\alpha$-β-5 to dimerize with FLAG-α-α-5 has implicated the N-terminal segment of the GAFa domains in the exclusive PDE6$\alpha\beta$ association. Further evidence was provided by the analysis of the chimeric PDEs, His-α_β-α-5 and His-β_α-β-5, containing short replacements PDE6β-57–72 and PDE6α-59–74 within the PDE6α and PDE6β GAF regions, respectively. PDE6β-57–72 and PDE6α-59–74 correspond to a region of PDE2GAFa, α1 helix-α1/α2 loop, that is involved in the PDE2 dimer interface (28). Not only did the replacements prevent heterodimerization between His-α_β-α-5 and myc-β-β-5, and between His-β_α-β-5 and FLAG-α-α-5, but His-α_β-α-5 gained the ability for self-dimerization and heterodimerization with FLAG-α-α-5. Dimerization of His-α_β-α-5 with FLAG-α-α-5 suggests that the lack of homodimerization of PDE6α is caused by a defect in the interaction between the two PDE6α-59–74 segments (Fig. 7*D*). However, homodimerization of His-α_β-α-5 coupled with the absence of association of His-β_α-β-5 with myc-β-β-5 indicates that the lack of homodimerization of PDE6β cannot be accounted for by the defective interaction between the two PDE6β-57–74 segments. Homology modeling of the PDE6$\alpha\beta$ GAFa dimer using the structure of PDE2GAFa dimer as a template indicates that PDE6β-57–72 may participate in two sets of interactions involving PDE6α-59–74 and PDE6α-216–224 (Fig. 7, *A–C*). PDE6α-216–224 resides at the start of the helix connecting GAFa and GAFb. Table I shows that no dimers had been formed that would entail the interaction between PDE6β-57–72 and the beginning of the connecting helix from PDE6β. Therefore, this structural constraint appears to disallow homodimerization of PDE6β (Fig. 7*D*). Additional negative dimerization determinants within the GAFa domain of PDE6β cannot be ruled out. A significant number of residues within PDE6α-59–74/PDE6β-57–72 and PDE6α-216–224/PDE6β-214–222 are not conserved (Fig. 7*B*) and may play a role in the selective assembly of PDE6$\alpha\beta$.

The finding that the selectivity determinants of PDE6 dimerization are confined to relatively short segments in the GAFa domains supports the feasibility of generating mutant PDE6 α and β subunits capable of homodimerization. Mutant homodimeric rod PDE6 expressed in transgenic animals would allow us to study the individual catalytic subunits and elucidate the functional significance of rod PDE6 heterodimerization.

REFERENCES

1. Chabre, M., and Deterre, P. (1989) *Eur. J. Biochem.* **179,** 255–266
2. Yarfitz, S., and Hurley, J. B. (1994) *J. Biol. Chem.* **269,** 14329–14332
3. Beavo, J. A. (1995) *Physiol. Rev.* **75,** 725–748

4. Francis, S. H., Turko, I. V., and Corbin, J. D. (2001) *Prog. Nucleic Acids Res. Mol. Biol.* **65,** 1–52
5. Baehr, W., Devlin, M. J., and Applebury, M. L. (1979) *J. Biol. Chem.* **254,** 11669–11677
6. Hurley, J. B., and Stryer, L. (1982) *J. Biol. Chem.* **257,** 11094–11099
7. Ovchinnikov, Y. A., Lipkin, V. M., Kumarev, V. P., Gubanov, V. V., Khramtsov, N. V., Akhmedov, N. B., Zagranichny, V. E., and Muradov, K. G. (1986) *FEBS Lett.* **204,** 288–292
8. Lipkin, V. M., Khramtsov, N. V., Vasilevskaya, I. A., Atabekova, N. V., Muradov, K. G., Li, T., Johnston, J. P., Volpp, K. J., and Applebury, M. L. (1990) *J. Biol. Chem.* **265,** 12955–12959
9. Li, T., Volpp, K., and Applebury, M. L. (1990) *Proc. Natl. Acad. Sci. U. S. A.* **87,** 293–297
10. Hamilton, S. E., and Hurley, J. B. (1990) *J. Biol. Chem.* **265,** 11259–11264
11. Florio, S. K., Prusti, R. K., and Beavo, J. A. (1996) *J. Biol. Chem.* **271,** 24036–24047
12. Cook, T. A., Ghomashchi, F., Gelb, M. H., Florio, S. K., and Beavo, J. A. (2001) *J. Biol. Chem.* **276,** 5248–5255
13. McAllister-Lucas, L. M., Sonnenburg, W. K., Kadlecek, A., Seger, D., Trong, H. L., Colbran, J. L., Thomas, M. K., Walsh, K. A., Francis, S. H., Corbin, J. D., and Beavo, J. A. (1993) *J. Biol. Chem.* **268,** 22863–22873
14. Gillespie, P. G., and Beavo, J. A. (1989) *Mol. Pharmacol.* **36,** 773–781
15. Turko, I. V., Ballard, S. A., Francis, S. H., and Corbin, J. D. (1999) *Mol. Pharmacol.* **56,** 124–130
16. Aravind, L., and Ponting, C. P. (1997) *Trends Biochem. Sci.* **22,** 458–459
17. Charbonneau, H., Prusti, R. K., LeTrong, H., Sonnenburg, W. K., Mullaney, P. J., Walsh, K. A., and Beavo, J. A. (1990) *Proc. Natl. Acad. Sci. U. S. A.* **87,** 288–292
18. Stroop, S. D., and Beavo, J. A. (1991) *J. Biol. Chem.* **266,** 23802–23809
19. Soderling, S. H., Bayuga, S. J., and Beavo, J. A. (1999) *Proc. Natl. Acad. Sci. U. S. A.* **96,** 7071–7076
20. Fawcett, L., Baxendale, R., Stacey, P., McGrouther, C., Harrow, I., Soderling, S., Hetman, J., Beavo, J. A., and Phillips, S. C. (2000) *Proc. Natl. Acad. Sci. U. S. A.* **97,** 3702–3707
21. Martins, T. J., Mumby, M. C., and Beavo, J. A. (1982) *J. Biol. Chem.* **257,** 1973–1979
22. Corbin, J. D., Turko, I. V., Beasley, A., and Francis, S. H. (2000) *Eur. J. Biochem.* **267,** 2760–2767
23. Rybalkin, S. D., Rybalkina, I. G., Feil, R., Hofmann, F., and Beavo, J. A. (2002) *J. Biol. Chem.* **277,** 3310–3317
24. Okada, D., and Asakawa, S. (2002) *Biochemistry* **41,** 9672–9679
25. Cote, R. H., Bownds, M. D., and Arshavsky, V. Y. (1994) *Proc. Natl. Acad. Sci. U. S. A.* **91,** 4845–4849
26. Mou, H., and Cote, R. H. (2001) *J. Biol. Chem.* **276,** 27527–27534
27. Thomas, M. K., Francis, S. H., and Corbin, J. D. (1990) *J. Biol. Chem.* **265,** 14964–14970
28. Martinez, S. E., Wu, A. Y., Glavas, N. A., Tang, X. B., Turley, S., Hol, W. G., and Beavo, J. A. (2002) *Proc. Natl. Acad. Sci. U. S. A.* **99,** 13260–13265
29. Kameni Tcheudji, J. F., Lebeau, L., Virmaux, N., Maftei, C. G., Cote, R. H., Lugnier, C., and Schultz, P. (2001) *J. Mol. Biol.* **310,** 781–791
30. Fink, T. L., Francis, S. H., Beasley, A., Grimes, K. A., and Corbin, J. D. (1999) *J. Biol. Chem.* **274,** 34613–34620
31. Richter, W., and Conti, M. (2002) *J. Biol. Chem.* **277,** 40212–40221
32. Fung, B. K.-K., Young, J. M., Yamane, H. K., and Griswold-Prenner, I. (1990) *Biochemistry* **29,** 2657–2664
33. Artemyev, N. O., Surendran, R., Lee, J. C., and Hamm, H. E. (1996) *J. Biol. Chem.* **271,** 25382–25388
34. Piriev, N. I., Yamashita, C., Samuel, G., and Farber, D. (1993) *Proc. Natl. Acad. Sci. U. S. A.* **90,** 9340–9344
35. Qin, N., and Baehr, W. (1994) *J. Biol. Chem.* **269,** 3265–3271
36. Granovsky, A. E., Natochin, M., McEntaffer, R. L., Haik, T. L., Francis, S. H., Corbin, J. D, and Artemyev, N. O. (1998) *J. Biol. Chem.* **273,** 24485–24490
37. Thompson, W. J., and Appleman, M. M. (1971) *Biochemistry* **10,** 311–316
38. Natochin, M., and Artemyev, N. O. (2000) *Methods Enzymol.* **315,** 539–554
39. Bradford, M. M. (1976) *Anal. Biochem.* **72,** 248–254
40. Porath, J. (1963) *Pure Appl. Chem.* **6,** 233–244
41. Laemmli, U. K. (1970) *Nature* **227,** 680–685
42. Martin, R. G., and Ames, B. N. (1961) *J. Biol. Chem.* **236,** 1372–1379
43. Siegel, L. M., and Monty, K. J. (1966) *Biochim. Biophys. Acta* **112,** 346–362
44. Guex, N., and Peitsch, M. C. (1997) *Electrophoresis* **18,** 2714–2723
45. Thompson, J. D., Higgins, D. G., and Gibson, T. J. (1994) *Nucleic Acids Res.* **22,** 4673–4680